

A Geometric Approach for the Comparison of Kinematic Synergy Postures

Federico Tessari

*Dept. of Mechanical Engineering
MIT
Cambridge, MA, USA
ftessari@mit.edu*

A. Michael West Jr.

*Dept. of Mechanical Engineering
Johns Hopkins University
Baltimore, MD, USA
awest36@jh.edu*

Neville Hogan

*Dept. of Mechanical Engineering
MIT
Cambridge, MA, USA
neville@mit.edu*

Abstract—The analysis of human movements has highlighted the presence of stereotyped coordination patterns among the different joints of the human body. These patterns are commonly referred to as kinematic synergies. Synergies have been used to both elucidate the underlying neuromotor control strategies adopted by humans during coordinated motion and inform the design and control of assistive and rehabilitative devices such as prostheses and exoskeletons. A particularly thorny problem in the analysis of synergies is the comparison of the synergy postures i.e., the hyper-dimensional vectors containing the contribution of each analyzed feature (e.g., joint angles) to the considered synergies. Often, synergy postures are compared using cosine similarity, which is sensitive to the dimensionality of the input data and does not offer an intuitive understanding of the synergies' similarities and differences. In this study, we introduce a new geometric method, Geometric Configuration Similarity (GCS), specifically designed to compare kinematic synergy postures, with a particular emphasis on hand kinematic synergies. GCS provides a more intuitive geometric understanding of how these postures relate to one another. We demonstrate its advantages over cosine similarity through experimental and numerical results, offering the human motor control and rehabilitation robotics communities a new tool for analyzing kinematic hand synergies and improving the design and control of assistive systems.

Index Terms—synergies, kinematics, hand, manipulation, dexterity, similarity

I. INTRODUCTION

The fine and dexterous control of the hand requires the coordination of a large number of joint degrees of freedom (20+) (i.e., hand joints), and more than double that number of intrinsic and extrinsic muscles of the hand [1], [2]. Given this complexity, the question arises: how do humans seamlessly control their hands without incurring the control limitations associated with the curse of dimensionality [3]? One of the leading theories assumes that humans might take advantage of lower-dimensional and sufficiently stereotyped commands to simplify the motor control problem. Such commands are often referred to as motor synergies, and depending on the considered physiological nature of the signals, they are usually classified as neural [4], [5], muscular [6] or kinematic synergies [7]–[10].

The seminal work by Santello et al. [4], [7] showed that a few kinematic synergies - typically extracted by means of dimensionality reduction techniques such as principal component analysis (PCA) [11] or singular value decomposition

(SVD) [12] - accounted for most of the variance in the data of healthy humans performing a variety of reaching and grasping movements. Subsequent work has found similar results in tasks that involve object manipulation [8], [13], [14] the American sign language [6], and even piano playing [10], [15]. For review see [16]. Moreover, some research has highlighted how such synergies are both the results of biomechanical constraints (e.g., tendons and ligaments), as well as descending neural commands [8], [17]. Additionally, research indicates that the reduction of the operational degrees of freedom of the hand may facilitate more straightforward control [18]–[22]. Prior work by the authors showed how humans need to recruit a growing number of synergies in order to perform more advanced dexterous manipulation tasks such as wire-harnessing or playing a musical instrument [10]. A recent theoretical framework highlighted how the number of synergies that humans can employ to perform a given motor task may exceed the number of controlled features, such as joint angles or muscle contractions [23]. Moreover, substantial efforts have been made to refine mathematical methods for extracting synergies [9], [24], [25] through various dimensionality reduction techniques [11], [12], [26].

However, a particularly thorny problem is represented by the difficulty of comparing the synergy vectors resulting from these reduction techniques. The synergy vectors or hyper-points are often high dimensional - with dozens if not hundreds of elements - which limits our capability to visualize and, consequently, get a profound insight on their relation to each other. A common approach to compare synergy vectors, specifically termed ‘synergy postures’ for kinematic synergies, is to compute the cosine similarity between them. The most widely used formulation computes the positive angle between two vectors, returning 0 if the vectors are orthogonal and 1 if the vectors are collinear.

Recent work by Tessari and Hogan highlighted how the cosine similarity metric is sensitive to the number of dimensions [27]. Specifically, for increasing dimensions the cosine similarity between any 2 random vectors will tend to converge to a value of about 0.75, with decreasing variance. This represents a substantial limitation to the use and interpretability of such a metric. An alternative approach would be to use a dimension-insensitive metric, such as the dimension insensitive Euclidian

metric (DIEM) [27]. This metric is unaffected by the number of dimensions, enabling robust statistical analysis and hypothesis testing—areas where cosine similarity falls short. However, DIEM relies on comparing synergy vectors that are not of unit length. This can be the case for muscular synergies extracted through Non-Negative Matrix Factorization [26], [28], [29], but not for kinematic synergies obtained through PCA or SVD. Moreover, most distance metrics still do not provide an intuitive way to visualize and internalize the similarity between kinematic synergies. To address the limitations of cosine similarity and DIEM, we propose a new geometric approach to compare kinematic hand synergies, called “Geometric Configuration Similarity”. This method, which maps kinematic synergies to task-space motion, enables users to quantitatively compare and visualize pairs of kinematic hand synergy postures. In the following sections, we demonstrate the shortcomings of cosine similarity while contrasting it with our proposed approach. Additionally, we provide a library for future researchers to implement the Geometric Configuration Similarity in their work.

II. MATERIALS AND METHODS

A. Synergy Extraction through SVD

Consider a matrix $X \in \mathbb{R}^{n \times m}$ containing the kinematic data of the joint trajectories recorded across n observations (e.g., the time evolution of each degree of freedom) and m number of features (e.g., the number of analyzed degrees of freedom, DoF) for a given set (one or more) of experiments.

According to West et al. [9], prior to synergy extraction the data should be centered i.e., the mean value of each column - which represents the average angular value for that DoF - needs to removed. This is done to prevent the first synergy from incorrectly ‘aiming’ toward the center of the offset data distribution.

$$X^* = X - \text{mean}(X) \quad (1)$$

Then, synergies can be extracted using SVD — the most adopted algorithm for kinematic synergy extraction [7], [8] — on the mean-removed data set:

$$X^* = U \cdot S \cdot V^T \quad (2)$$

where $U \in \mathbb{R}^{n \times n}$ is an orthonormal matrix whose columns denote the temporal evolution of a given synergy, $S \in \mathbb{R}^{n \times m}$ is diagonal matrix of singular values which give an estimate of the Variance-Accounted-For (VAF) in a given synergy, and $V \in \mathbb{R}^{m \times m}$ is an orthonormal matrix whose columns represent the synergy vectors $V = [\mathbf{v}_1, \mathbf{v}_2, \dots, \mathbf{v}_m]$. The elements of each synergy vector represent the contribution of each DoF to that synergy $\mathbf{v}_i = [\theta_1, \theta_2, \dots, \theta_m]^T$. The synergy vectors \mathbf{v}_i are of unitary length. For a geometrical interpretation of this, see [9]. In the specific case of hand joint kinematic synergies, the elements of \mathbf{v}_i represent the proportion by which each joint of the hand contributes to that synergy.

B. Limitations of Cosine Similarity

Comparing a pair of synergy vectors $\mathbf{v}_i, \mathbf{v}_j$ fundamentally requires establishing a distance metric between these two hyper-dimensional quantities. As briefly mentioned in the Introduction, this is often done by computing the cosine similarity between them:

$$\cos(\phi) = \frac{|\mathbf{v}_i^T \cdot \mathbf{v}_j|}{\|\mathbf{v}_i\| \cdot \|\mathbf{v}_j\|} \quad (3)$$

However, Tessari et al. showed that this metric is **sensitive to the number of dimensions** and, thus, is not able to provide statistically reliable comparisons [27]. Specifically, as the number of dimensions grows the cosine similarity of two randomly generated vectors tends toward 0.75. Moreover, the resulting computation does **not provide an intuitive geometrical understanding** of how the posture of the hand differs between the two synergy vectors.

C. Geometric Configuration Similarity

To address the limitations of the cosine similarity metric—namely (i) dimension-sensitivity, and (ii) geometric interpretability—the authors propose a new approach coined ‘Geometric Configuration Similarity’ (GCS), to compute the degree of similarity or difference between any two pairs of kinematic synergy vectors \mathbf{v}_i , and \mathbf{v}_j . The approach is showcased for hand kinematic synergies, but its application extends to any form of kinematic synergies at every level of the human body.

The core idea of the GCS is to map the synergy vectors from the joint-space to the task-space. This mapping is biomechanically informed through direct kinematics. Given a specific geometry of the hand (i.e., link lengths and joint types) the mapping of any point \mathbf{p} on the hand with respect to a set of joint coordinates—assumed here to be the relative angles between successive links—is unique and well defined as:

$$\mathbf{p} = \mathcal{L}(\Theta) = \mathcal{L}(\theta_1, \dots, \theta_m) \quad (4)$$

where \mathcal{L} describes the forward kinematics.

To map a synergy vector \mathbf{v}_i to a hand task-space configuration, we need to (i) multiply it by an activation coefficient u —which could also be a function, $u(t)$, if the intention is to reconstruct the entire motion—and (ii) add back the previously subtracted average posture of the original dataset $\Theta_{avg} = \text{mean}(X)$:

$$\Theta_i = u \cdot \mathbf{v}_i + \Theta_{avg} \quad (5)$$

Together, Equations 4 and 5, allow for the mapping of a synergy vector to any point of the considered geometry (e.g., the hand).

In the proposed case (i.e., hand kinematic synergies), we considered a 20 DoFs hand model characterized by 4 DoFs per finger. For the index, middle, ring and little fingers, we included flexion-extension of the metacarpophalangeal (MCP), proximal interphalangeal (PIP), and distal interphalangeal

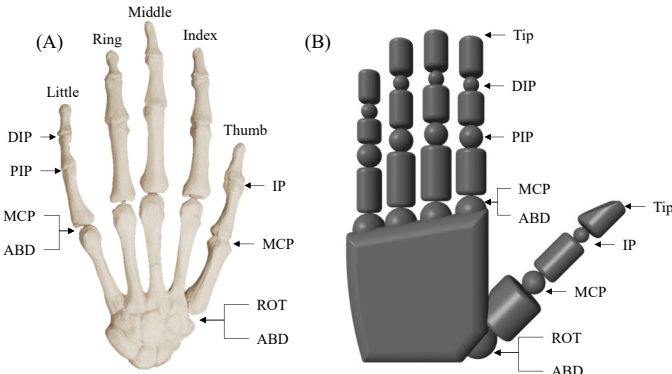


Fig. 1. Adopted hand model. Panel (A) shows the considered human anatomical joints. Panel (B) presents the reconstructed rigid link model.

(DIP) joints, and abduction-adduction (ABD) of the metacarpophalangeal joint. For the thumb, we included rotation (ROT) and abduction-adduction (ABD) at the carpometacarpal and flexion-extension at the metacarpophalangeal (MCP), and interphalangeal (IP) joints. Figure 1A provides a schematic representation of the considered anatomical hand joint.

A rigid-link model (Figure 1B), based on the aforementioned 20 DoFs, was developed considering the following two assumptions. First, the PIP and DIP joints of the index, middle, ring, and little fingers, along with the MCP and IP joints of the thumb, were modeled as perfect rotational joints. Second, the MCP and ABD joints of the index, middle, ring, and little fingers, as well as the ROT and ABD joints of the thumb, were modeled as universal joints (U-joints or Cardan joints).

The link lengths were sized considering the 50th percentile male hand size [30]. However, we want to emphasize that the proposed metric is not influenced by the size of the considered hand. Additional details are provided in the Discussion.

Considering the presented hand model and the mapping from joint-space to task-space using Equations 4 and 5, the ‘Geometric Configuration Similarity’ fundamentally computes the Euclidean distance between a pair of hand configurations from two synergy vectors $\mathbf{v}_i, \mathbf{v}_j$. The Euclidian distance is computed at 3 different key-points for each finger. Specifically, for the index, middle, ring and little fingers the Cartesian coordinates of the PIP joint, DIP joint and tip of the finger are considered; for the thumb, the MCP joint, IP joint and tip of the thumb are considered. These distances are normalized by the maximum distance that each key-point can assume considering the biomechanical range of motion (ROM) limits of each joint of the hand. The ROM for each joint were extracted from the works of: Bain et al. for the index, middle, ring and little MCP, DIP, and PIP joints [31], Gracia-Ibanez et al. for the ROT, MCP, and IP joints of the thumb [32], and from available online data sheets for the ABD joints [33].

This normalization provides two advantages: (i) it ensures that the size of the hand will not influence the proposed metric, (ii) it guarantees a finite range for the metric, namely 0 to 100.

Mathematically, the Geometric Configuration Similarity between two task-space mapped synergy vectors Θ_i, Θ_j is for-

mulated as:

$$GCS(f) = \frac{1}{3} \sum_{k=1}^3 100 \cdot \left(1 - \frac{\|\mathbf{p}_k(\Theta_i) - \mathbf{p}_k(\Theta_j)\|_2^2}{\max(d(k, f))} \right) \quad (6)$$

with $f = 1, \dots, 5$

Where f represents the finger index, and k is the key-point index. $\mathbf{p}_k(\Theta_i)$, and $\mathbf{p}_k(\Theta_j)$ are, respectively, the task-space Cartesian positions of the k -th key-point for the synergy vector \mathbf{v}_i and \mathbf{v}_j . $\max(d(k, f))$ is the maximum Euclidean distance that the k -th key-point of the f -th finger can assume considering the human physiological ROM [31]–[33]. Note, GCS produces a similarity measure for each of the five fingers.

Intuitively, for a given finger f , if the two synergy vectors map to the exact same position, their distance will be $\|\mathbf{p}_k(\Theta_i) - \mathbf{p}_k(\Theta_j)\|_2^2 = 0 \forall k$, and therefore the Geometric Configuration Similarity will be 100. Alternatively, if the two synergy vectors map to the maximum possible biomechanical distance $\|\mathbf{p}_k(\Theta_i) - \mathbf{p}_k(\Theta_j)\|_2^2 = \max(d(k, f)) \forall k$, then the Geometric Configuration Similarity will be 0.

To provide a unique scalar macroscopic description of the similarity between two synergy vectors, we can use the arithmetic mean of the Geometric Configuration Similarities of the five fingers:

$$\text{mean}(GCS) = \frac{1}{5} \sum_{f=1}^5 GCS(f) \quad (7)$$

D. The Selection of the Activation Coefficients

Particular attention must be given to the selection of the activation coefficient u . As presented in Equation 5, the activation coefficient is necessary to map the synergy vector to a given joint configuration or trajectory. In fact, without an activation coefficient, the synergy vectors just inform us of the proportionality ratio between features but not the extent to which such synergies are employed. Several options for the selection of u are possible. However, for the sake of comparing synergies, two main approaches are considered here.

The first approach consists in using the maximum and minimum activation coefficients found in the columns of the matrix product $U \cdot S = T$, found in Equation 2. The resulting matrix $T = [\mathbf{t}_1, \mathbf{t}_2, \dots, \mathbf{t}_m]$ will have as columns the temporal evolutions of each synergy vector based on the input data X^* . Consequently, the $\min(t)$ and $\max(t)$ values of each temporal evolution represent the maximum and minimum values that a given synergy assumed based on the input data.

This approach is data-driven and, therefore, eliminates the risk of over-activating a synergy vector with respect to another one. Moreover, it will always generate physiologically reasonable movements - assuming no errors during data acquisition.

However, one should remember that by using PCA or SVD, the synergies are extracted in decreasing order of variance-accounted-for. Therefore, higher order synergies will have smaller activation coefficients, and this will influence the comparability of synergy vectors with different orders.

Moreover, if interested in reconstructing the entire motion, you can use these activation coefficients to craft a personalized temporal evolution. In the provided software package, a 4th order polynomial (sine-wave like) starting at 0 and stopping at 0 and passing through $\max(t)$ and $\min(t)$ was adopted.

The second approach is instead driven by biomechanics. Instead of using the activation coefficients extracted through PCA/SVD, these can be modeled so that a synergy vector spans the maximum range of motion of a certain feature. A reasonable choice is to select the largest element of a synergy vector i.e., the largest contributing joint DoF in the hand case, and scale it such that its value will reach the minimum and maximum ROM of that hand joint. In this case, the activation functions for higher order synergies will not be limited by the lower variance-accounted-for synergies. However, it is not guaranteed that the resulting hand posture will represent a physiological configuration.

The authors think the selection of the appropriate activation function is context dependent. In the case of comparison with experimental data, the first approach i.e., using the columns of T , seems more appropriate, and that is what is used in the Results of this work. In the case of using synergies for design or control purposes, the second approach i.e., extending the synergy to the ROM limits, might be the right choice.

E. The three Geometric Configuration Similarities

Considering two synergy vectors \mathbf{v}_i , and \mathbf{v}_j extracted from dataset having average postures $\Theta_{i_{avg}}$, and $\Theta_{j_{avg}}$, and with minimum and maximum activation coefficients u_{max_i} , u_{max_j} , u_{min_i} , and u_{min_j} , three different, Geometric Configuration Similarities are computed. These represent the average posture, maximum posture and minimum posture conditions:

$$GCS(f)_{avg}|\Theta_i = \Theta_{i_{avg}} \wedge \Theta_j = \Theta_{j_{avg}} \quad (8)$$

$$GCS(f)_{max}|\Theta_i = u_{max_i} \cdot \mathbf{v}_i + \Theta_{i_{avg}} \wedge \quad (9)$$

$$\begin{aligned} \Theta_j &= u_{max_j} \cdot \mathbf{v}_j + \Theta_{j_{avg}} \\ GCS(f)_{min}|\Theta_i &= u_{min_i} \cdot \mathbf{v}_i + \Theta_{i_{avg}} \wedge \quad (10) \\ \Theta_j &= u_{min_j} \cdot \mathbf{v}_j + \Theta_{j_{avg}} \end{aligned}$$

The $GCS(f)_{avg}$ provides information on how much the average postures of the considered datasets are similar to each other. This parameter is independent of the considered synergy vectors and it is always equal to 100 when the comparison is performed between synergies extracted from the same dataset i.e., $\Theta_i = \Theta_j$. $GCS(f)_{max}$ and $GCS(f)_{min}$ quantify the geometric difference between the maximum or minimum postures between the considered synergy vectors.

Two different applications of the Geometric Configuration Similarity are reported in the following. The first presents a numerical example involving two biomechanically relevant, artificially synthesized hand postures that yield a GCS close to the minimum. This example highlights a disparity between GCS and cosine similarity. The second provides an experimental example, consisting of two case studies, and applies

the GCS to the kinematic hand synergies extracted from the authors' previously reported work on piano playing [10].

A software package to run GCS and reproduce the experimental results presented in this work can be found at the following GitHub repository: <https://github.com/ftessari23/GCS>.

III. RESULTS

The hand model was calibrated on the 50th percentile male hand, and the resulting maximum distances $\max(d(k, f))$ for each key-point (PIP,DIP,Tip) and each finger are reported in Table III.

$\max(d(k, f))$ [m]	Joints		
	Tip	DIP (IP)	PIP (MCP)
Thumb	0.195 ± 0.003	$0.159 \pm < 0.001$	$0.083 \pm < 0.001$
Index	0.176 ± 0.003	0.126 ± 0.002	$0.071 \pm < 0.001$
Middle	0.193 ± 0.003	0.144 ± 0.003	$0.085 \pm < 0.001$
Ring	0.194 ± 0.002	0.149 ± 0.002	$0.086 \pm < 0.001$
Little	0.170 ± 0.003	0.126 ± 0.002	$0.076 \pm < 0.001$

TABLE I
MAXIMUM EUCLIDEAN DISTANCE PLUS-MINUS THE NUMERICAL MEASUREMENT TOLERANCE AT EACH KEY-POINT (PIP, DIP, TIP) IN EACH FINGER. IN BRACKETS YOU CAN FIND THE NAME OF THE THUMB JOINTS.

A. Numerical Example: Joints Limit Hand Configurations

In this first example, we aimed to compare the most biologically distinct hand postures. Thus, we chose two hand configurations in which the first has all the joints at the maximum ROM and, the second has all the joints at the minimum ROM:

$$\Theta_1 = [\theta_{1_{max}}, \dots, \theta_{20_{max}}] \quad (11)$$

$$\Theta_2 = [\theta_{1_{min}}, \dots, \theta_{20_{min}}] \quad (12)$$

The cosine similarity between these biomechanically distinct hand postures is 0.71, which corresponds to an angular difference of about 44.6°. This suggests a non-negligible similarity between the vectors.

However, when the vectors are mapped to the task-space and the GCS is computed, we observe (Figure 2) that the 2 postures have very poor similarity - as expected - with an average GCS of 8.7% across the five fingers. It is worth emphasizing that, despite the very small value, the GCS did not converge completely to 0%. This is expected, since the maximum and minimum ROM do not always represent the condition of maximum Euclidean distance for each of the different finger key-points.

B. Experimental Example: Piano Playing

Next, we compare kinematic synergies extracted on a group of healthy individuals while performing a series of piano pieces. All subjects were right-handed, received a comprehensive briefing on the experimental procedures, and signed a consent form approved by MIT's Institutional Review Board. We invite readers to refer to the work by West et al. for details on the experimental data acquisition and processing [10]. Here, two case studies are considered to highlight the benefits of the Geometric Configuration Similarity.

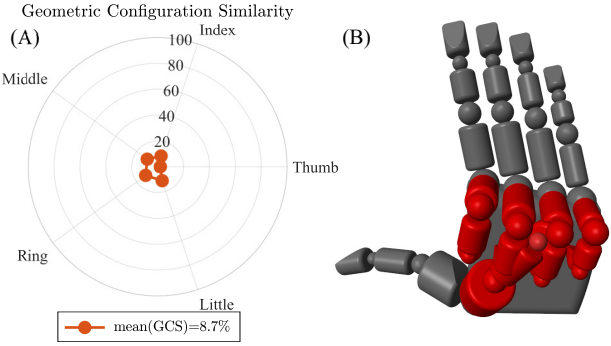


Fig. 2. Geometric Configuration Similarity between two synthetic synergy vectors \mathbf{v}_1 and \mathbf{v}_2 obtained by having the hand joints at their maximum and minimum ROM, respectively. In panel (A), the orange, dotted polygon represents the comparison between the two hand configuration postures $GCS(f)$. In panel (B), the maximum hand postures $\Theta_{1\max}(\mathbf{v}_1)$ and $\Theta_{2\max}(\mathbf{v}_2)$ are reported in the 3D hand model in gray and red, respectively.

1) Within-Subject - Different Order Synergies: In the first case study, we present a comparison of the first 2 kinematic synergies of a representative subject (nr. 2) performing the Bach Prelude in C Major by J.S. Bach. The synergies were extracted using the approach presented in Section II.A; they represent the first 2 columns of matrix V (i.e., \mathbf{v}_1 and \mathbf{v}_2). They account, respectively, for 44% and 25% of the Variance-Accounted-For (VAF). By computing the cosine similarity of these two synergies, we observe that such synergies are perfectly orthogonal:

$$\cos(\theta) = \frac{|\mathbf{v}_1^T \cdot \mathbf{v}_2|}{\|\mathbf{v}_1\| \cdot \|\mathbf{v}_2\|} = 0 \quad (13)$$

This follows directly from SVD, as the columns of V are orthonormal, meaning they are mutually orthogonal.

However, when using the Geometric Configuration Similarity, we observe (Figure 3) that the two synergies - despite their orthogonality - present substantial similarities. Specifically, the maximum and minimum postures of the first 2 synergies show an average Geometric Configuration Similarity across the five fingers of 71.2% and 82.4%, respectively. The average posture Θ_{avg} presents, instead, a GCS of 100%. This is a natural consequence of the fact that both synergies were extracted from the same dataset, thus they must have the same average posture.

2) Between-Subjects - Same Order Synergies: In the second case study, we compare the first synergies of two different subjects (nr. 2 and nr. 5) performing the same piano piece (i.e., Bach Prelude in C Major). These two synergies account, respectively, for 44% and 42% of the Variance-Accounted-For. Their cosine similarity is equal to 0.19, which represents an angular difference of about 79° . Once more, the synergies appear close to orthogonality, and thus would typically be considered very *different postures*.

However, when the synergies are compared with the Geometric Configuration Similarity, we observe (Figure 4) that the average postures present an average GCS of 89.4% indicating that the two subjects had a similar - but not identical -

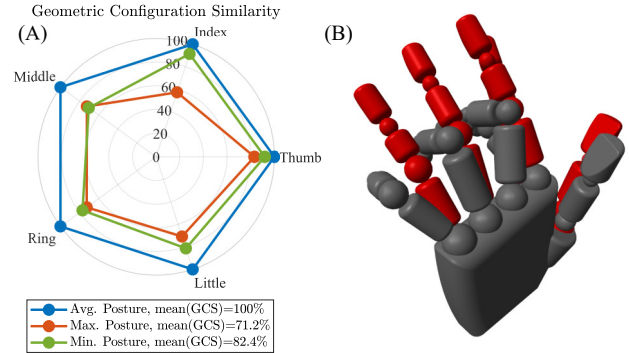


Fig. 3. Geometric Configuration Similarity between the first two synergy vectors, \mathbf{v}_1 and \mathbf{v}_2 , of a representative subject playing the piano piece Bach Prelude in C Major. In panel (A), the blue, dotted polygon represents the comparison between average postures $GCS(f)_{avg}$, the orange, dotted polygon is the comparison between maximum postures $GCS(f)_{max}$, and the green, dotted polygon is the comparison between minimum postures $GCS(f)_{min}$. In panel (B), the maximum hand postures $\Theta_{1\max}(\mathbf{v}_1)$ and $\Theta_{2\max}(\mathbf{v}_2)$ are reported in the 3D hand model in gray and red, respectively.

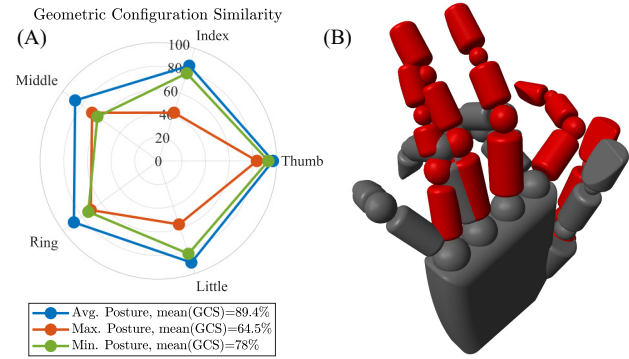


Fig. 4. Geometric Configuration Similarity between the first synergy vectors \mathbf{v}_{1s2} and \mathbf{v}_{1s5} of two representative subjects (nr. 2 and nr. 5) performing the same piano playing task i.e., Bach Prelude in C Major. In panel (A), the blue, dotted polygon represents the comparison between average postures $GCS(f)_{avg}$, the orange, dotted polygon is the comparison between maximum postures $GCS(f)_{max}$, and the green, dotted polygon is the comparison between minimum postures $GCS(f)_{min}$. In panel (B), the maximum hand postures $\Theta_{1\max}(\mathbf{v}_{1s2})$ and $\Theta_{1\max}(\mathbf{v}_{1s5})$ are reported in the 3D hand model respectively in gray and red, respectively.

average hand configuration while playing the same piano piece. Moreover, the maximum and minimum hand postures - dictated by each subjects' first synergy - show an average GCS of 64.5% and 78%, respectively. These values provide a geometrically intuitive understanding of how *similar* the two synergies between the subjects are. Moreover, this tool enables us to observe that the index and little fingers are actually the ones that were used most differently between the subjects (see Figure 4).

IV. DISCUSSION

In this paper, we addressed the limitations of cosine similarity by proposing a novel geometric approach for comparing kinematic hand synergies, termed Geometric Configuration Similarity (GCS). GCS utilizes MATLAB's multibody simulation, Simscape, and forward kinematics to map joint space

synergies to a task-space hand configuration. This mapping enables both visual and analytical comparison of kinematic synergies. Through numerical and experimental comparisons, we demonstrate that GCS provides valuable insights overlooked by cosine similarity. Looking ahead, we believe that the publicly available GCS framework will assist researchers in conducting more thorough analyses of hand kinematics.

A. Geometric Interpretability

1) *Numerical Example:* In our numerical example, we compared two biologically distinct hand configurations: one with all joints at their maximum range of motion (ROM) and another with all joints at their minimum ROM. The Geometric Configuration Similarity (GCS) metric revealed a stark contrast between these two postures, yielding a low similarity score of 8.7% across the five fingers (Fig. 2). This finding highlights the significant differences in hand kinematics that are present, despite the similarity suggested by the cosine similarity score of 0.71. Such a high cosine similarity value implies significant similarity, which is misleading given that the two configurations are functionally and anatomically disparate.

This discrepancy underscores the limitations of relying solely on cosine similarity for evaluating hand postures. While cosine similarity may indicate a non-negligible relationship between the two synergy vectors, it fails to capture the true geometric differences that GCS effectively elucidates. By mapping the synergy vectors to task-space configurations, GCS provides a more intuitive representation of the distinct hand postures, thereby enhancing our understanding of the complex mechanics involved in hand manipulation.

It is important to note that in this numerical example, the GCS did not reach a minimum value of zero; instead, it was 8.7% (Fig. 2). While it may be theoretically possible to achieve a lower GCS, attaining a value of zero is unlikely. As outlined in Eq. 6, the Cartesian distance between each pair of keypoints is normalized by its theoretical maximum, which considers the biomechanical range of motion. For the GCS to equal zero, all keypoints would need to be positioned at points of maximum distance simultaneously. However, due to the interconnected nature of finger joints in our multibody model, the position of each keypoint is influenced by the configuration of the distal joints. Consequently, a configuration that maximizes the distance between the PIP and DIP joints may not necessarily maximize the distance at the TIP. This issue becomes even more pronounced when considering movements such as abduction and adduction. Nevertheless, Fig. 2 provides a useful reference for understanding the range of GCS values achievable under different configurations.

2) *Experimental Example:* In our first experimental example (*Within-Subject - Different Order Synergies*), we examined the kinematic synergies of a subject performing the Bach Prelude in C Major, focusing on the first two synergy vectors extracted via Singular Value Decomposition. While cosine similarity indicates that these two vectors are orthogonal, signifying that they span completely different hyperspaces—a

result of the SVD design—Geometric Configuration Similarity reveals significant kinematic similarities in the configuration space. This distinction is crucial, and it, again, underscores the limitations of relying solely on cosine similarity to evaluate hand postures. Moreover, GCS allows for a more intuitive interpretation of the data, enabling us to easily identify which fingers exhibit higher or lower similarity between the synergies. For example, in Fig. 3 we can see that the largest discrepancy lies in the motion of the index finger, whose maximum posture GCS is 57%, while there is high similarity in the thumb whose minimum and maximum posture GCS are 92% and 83%, respectively. Such insights are vital when discussing the functional roles of each synergy in hand movements. Consequently, one could argue that GCS serves as a valuable proxy measure for assessing the similarity of kinematic synergies as they relate to function, providing a deeper understanding of the intricacies of hand manipulation.

In our second experimental example (*Between-Subjects - Same Order Synergies*), we compared the first synergy vectors of two different subjects performing the same piano piece, the Bach Prelude in C Major. Notably, the cosine similarity for these vectors was measured at 0.19, indicating a relatively higher degree of similarity compared to the first example, where cosine similarity was 0 for within-subject comparisons of different order synergies. However, the Geometric Configuration Similarity tells a different story. In this case, the GCS for the maximum posture scenario decreased from 71.2% in the within-subject example to 64.5% when comparing between subjects, and similarly dropped from 82.4% to 78% in the minimum posture scenario. This juxtaposition highlights the limitations of cosine similarity and shows that GCS provides a more nuanced understanding of the functional similarities and differences in hand configurations. Moreover, GCS intuitively highlights that index and little finger motion might be the root of this cause; their maximum posture GCS reduced from 57%, index, and 71%, little, (Fig. 3) to 43% and 56% (Fig. 4), respectively. Such insights are critical for assessing how different individuals may employ similar synergies in varied ways during complex motor tasks.

B. Methodological Considerations

We want to highlight that the choice to utilize three key points per finger in measuring configuration was intentional and is crucial for eliminating discrepancies that may arise from redundancy in joint movements. For instance, if we were to measure only the distance at the Tip of each finger, that position could be achieved through multiple joint configurations. Specifically, the fingertip is described by three Cartesian degrees of freedom (DOF), while the finger possesses 4 (three flexion + 1 ab/adduction) DOFs, resulting in a one-dimensional null space. This means that different combinations of joint angles could yield the same TIP position, leading to ambiguity in interpreting movement. By selecting three key points—namely the PIP, DIP, and TIP, we increase the number of task-space DOFs relative to joint-space DOFs. This approach effectively eliminates the potential for errors due to

redundancy, and enhances the reliability of the GCS metric in capturing the complexities of hand movements.

The current version of the GCS is implemented in Matlab 2023b by using the multibody library available in Simulink/Simscape. However, alternatives exist. The first is to use Exp[licit], a recently released robotic control library, which has demonstrated better computational efficiency compared to standard robotic control toolboxes [34]. A second alternative is represented by advanced physics simulators such as Mujoco [35]. It is worth emphasizing that GCS is independent of the adopted software framework and is only a function of the considered hand geometry.

C. Limitations

One limitation of this study lies in the geometric assumptions regarding the hand model used for analyzing kinematic synergies. The model was based on a rigid-link representation of a 20-degree-of-freedom hand, incorporating four degrees of freedom per finger. However, more detailed mechanical models could be used to include the hand's remaining degrees of freedom [36]. Additionally, the current model may not adequately account for individual anatomical variations among subjects (e.g., larger or smaller hands, as well as different proportions between the phalanges), which could influence the accuracy of the Geometric Configuration Similarity (GCS) measurements. To help mitigate these limitations, we have open-sourced the GCS framework, allowing future researchers to utilize the metric and customize the hand model to better fit the specific anatomical characteristics of their study populations. Moreover, we are planning to parameterize the GCS model so that users will be able to input the hand percentile and automatically scale the GCS to the size of interest.

Another limitation of this study is the inability of GCS to provide statistical measures. In this regard, cosine similarity also falls short. As noted in our previous study [27], cosine similarity tends to converge toward 0.75, as the number of dimensions increases. DIEM addresses this issue [27], but requires non-unitary length vectors. Therefore, DIEM can be applied to either the reconstructed joint configurations (Equation 5) or the task-space positions (Equation 4). Future work should investigate the statistical properties of GCS and DIEM to enhance reliability and interpretability.

D. Impact

The discrepancies observed between cosine similarity and Geometric Configuration Similarity (GCS) can be attributed to the inherent differences in what each metric measures. Cosine similarity evaluates the angle between vectors, providing insight into their orientation rather than their geometric relationship in configuration space. This can lead - as shown in this paper - to misleading interpretations that fail to capture the intricate functional differences that exist between hand configurations, potentially obscuring the understanding of how specific movements contribute to overall hand function.

In contrast, GCS is inherently linked to the function of hand movements, as it assesses geometric distances between

mapped configurations in task space. This metric provides insights into how individual joint positions relate to functional outcomes in hand manipulation. By focusing on spatial configurations, GCS reveals critical kinematic similarities and differences essential for understanding motor control. For instance, it allows researchers to identify which fingers demonstrate higher or lower similarity in their movements, thus connecting the analysis of synergies to their functional roles.

This relationship highlights the utility of GCS in rehabilitation and motor control research, offering a more meaningful understanding of how hand movements serve specific functional objectives. For example, the GCS could be used as an input for the design of exoskeletal or prosthetic devices [37], [38] that aim to reconstruct specific hand motions e.g., piano playing or tool-use. Often times synergy orthogonality (observed through cosine similarity) is used to introduce a new DOF in assistive or rehabilitative devices. GCS offers a much more direct intuition of the geometric consequences of adding a new synergy to a certain hand configuration, thus enabling more adequate design choices. Additionally, GCS could be used as a metric to assess the recovery of hand motor function when computed between healthy and impaired individuals.

Finally, it is important to underline that the Geometric Configuration Similarity approach can be extended beyond hand kinematics to other parts of the human body such as upper-limb or lower-limb kinematic synergies.

Comparing GCS and cosine similarity offers an interesting parallel to a classic question in motor control: do humans plan and execute motion using intrinsic or extrinsic coordinates [39]–[41]? Cosine similarity, by comparing synergy vectors based on joint configurations, inherently reflects comparisons in intrinsic coordinates. This perspective has been used to discuss how humans may simplify the highly redundant motor control problem when planning an action. On the other hand, GCS compares synergies after projecting them into task-space, which corresponds to the end-effector positions and represents the extrinsic coordinates in which actions are typically executed. A substantial body of evidence suggests that humans often plan motion in extrinsic coordinates [39]–[41], where the focus is on achieving goals in the environment rather than coordinating individual joints. Therefore, future work using GCS could provide valuable insights into how humans simplify path planning in extrinsic coordinates, shedding light on how synergies are organized for task-level control.

V. CONCLUSIONS

The human hand, with its high degrees of freedom and ability to perform a vast array of complex tasks, poses significant challenges for studying its kinematics and motor control [36]. To simplify this analysis and enhance understanding, researchers have turned to the concept of synergies [16]. Cosine similarity has traditionally been the go-to method for comparing these synergies. However, as highlighted in this paper, cosine similarity has notable limitations, particularly when it comes to its interpretability and capturing the true

geometric relationships between hand configurations. To address these shortcomings, we introduced the Geometric Configuration Similarity (GCS) metric, a tool designed to provide researchers with a more intuitive and meaningful way to compare kinematic synergies. GCS can help researchers gain a deeper understanding of hand function, ultimately advancing the study of hand motor control in both healthy and impaired populations.

ACKNOWLEDGMENT

This work was funded by the Eric P. and Evelyn E. Newman fund, Takeda Fellowship, Accenture Fellowship, and the Johns Hopkins University Provost's Postdoctoral Fellowship.

REFERENCES

- [1] E. J. Alpenfels, "The anthropology and social significance of the human hand," *Artificial Limbs*, vol. 2, pp. 4–21, 1955.
- [2] C. L. Taylor and R. J. Schwarz, "The anatomy and mechanics of the human hand," *Artificial Limbs*, vol. 2, pp. 22–35, 1955.
- [3] R. Bellman, "Dynamic programming," *Science*, vol. 153, pp. 34–37, 7 1966.
- [4] M. Santello, G. Baud-Bovy, and H. Jörntell, "Neural bases of hand synergies," *Frontiers in Computational Neuroscience*, vol. 7, p. 42740, 3 2013.
- [5] V. C. Cheung and K. Seki, "Approaches to revealing the neural basis of muscle synergies: A review and a critique," *Journal of Neurophysiology*, vol. 125, pp. 1580–1597, 5 2021.
- [6] E. J. Weiss and M. Flanders, "Muscular and postural synergies of the human hand," *Journal of Neurophysiology*, vol. 92, pp. 523–535, 7 2004.
- [7] M. Santello, M. Flanders, and J. F. Soechting, "Postural hand synergies for tool use," *Journal of Neuroscience*, vol. 18, pp. 10105–10115, 12 1998.
- [8] E. Todorov and Z. Ghahramani, "Analysis of the synergies underlying complex hand manipulation," *Annual International Conference of the IEEE Engineering in Medicine and Biology - Proceedings*, vol. 26 VI, pp. 4637–4640, 2004.
- [9] A. M. West, F. Tessari, and N. Hogan, "The study of complex manipulation via kinematic hand synergies: The effects of data pre-processing," *IEEE ... International Conference on Rehabilitation Robotics : [proceedings]*, vol. 2023, pp. 1–6, 9 2023.
- [10] ——, "The study of dexterous hand manipulation: A synergy-based complexity index," *IEEE Transactions of Medical Robotics and Bionics*, 2024.
- [11] K. Pearson, "Principal components analysis," *The London Edinburgh and Dublin Philosophical Magazine and Journal of Science*, vol. 6, p. 559, 1901.
- [12] G. W. Stewart, "On the early history of the singular value decomposition," *SIAM review*, vol. 35, pp. 551–566, 7 2006.
- [13] A. M. West, "Towards a non-invasive measurement of human motion, force, and impedance during a complex physical-interaction task : wire-harnessing," 2020.
- [14] A. M. West Jr, "All Models are Wrong , Simple Models Provide Insight : A Study of Human Manipulation," Ph.D. dissertation, Massachusetts Institute of Technology, 2024.
- [15] S. Furuya, M. Flanders, and J. F. Soechting, "Hand kinematics of piano playing," *Journal of Neurophysiology*, vol. 106, pp. 2849–2864, 12 2011.
- [16] M. Santello, M. Bianchi, M. Gabiccini, E. Ricciardi, G. Salvietti, D. Prattichizzo, M. Ernst, A. Moscatelli, H. Jörntell, A. M. Kappers, K. Kyriakopoulos, A. Albu-Schäffer, C. Castellini, and A. Bicchi, "Hand synergies: Integration of robotics and neuroscience for understanding the control of biological and artificial hands," pp. 1–23, jul 2016.
- [17] M. H. Schieber and M. Santello, "Hand function: peripheral and central constraints on performance," *Journal of applied physiology*, vol. 96, pp. 2293–2300, 6 2004.
- [18] T. Flash and B. Hochner, "Motor primitives in vertebrates and invertebrates," pp. 660–666, dec 2005.
- [19] J. N. Ingram, K. P. Körding, I. S. Howard, and D. M. Wolpert, "The statistics of natural hand movements," *Experimental Brain Research*, vol. 188, no. 2, 2008.
- [20] S. A. Overduin, A. D'Avella, J. Roh, and E. Bizzi, "Modulation of muscle synergy recruitment in primate grasping," *Journal of Neuroscience*, vol. 28, no. 4, 2008.
- [21] S. A. Overduin, A. D'Avella, J. M. Carmena, and E. Bizzi, "Microstimulation Activates a Handful of Muscle Synergies," *Neuron*, vol. 76, no. 6, 2012.
- [22] S. A. Overduin, A. D'Avella, J. Roh, J. M. Carmena, and E. Bizzi, "Representation of muscle synergies in the primate brain," *Journal of Neuroscience*, vol. 35, no. 37, 2015.
- [23] F. Tessari, A. West, and N. Hogan, "On human motor coordination: The synergy expansion hypothesis," *bioRxiv*, p. 2024.04.10.588877, 4 2024.
- [24] N. Lambert-Shirzad and H. F. V. D. Loos, "Data sample size needed for analysis of kinematic and muscle synergies in healthy and stroke populations," *IEEE International Conference on Rehabilitation Robotics*, pp. 777–782, 8 2017.
- [25] K. Zhao, Z. Zhang, H. Wen, and A. Scano, "Number of trials and data structure affect the number and components of muscle synergies in upper-limb reaching movements," *Physiological Measurement*, vol. 43, p. 105008, 10 2022.
- [26] Y. X. Wang and Y. J. Zhang, "Nonnegative matrix factorization: A comprehensive review," *IEEE Transactions on Knowledge and Data Engineering*, vol. 25, pp. 1336–1353, 6 2013.
- [27] F. Tessari and N. Hogan, "Surpassing cosine similarity for multidimensional comparisons: Dimension insensitive euclidean metric (diem)," *arXiv*, 7 2024.
- [28] M. F. Rabbi, C. Pizzolato, D. G. Lloyd, C. P. Carty, D. Devaprakash, and L. E. Diamond, "Non-negative matrix factorisation is the most appropriate method for extraction of muscle synergies in walking and running," *Nature Scientific Reports*, 2020.
- [29] M. W. Berry, M. Browne, A. N. Langville, V. P. Pauca, and R. J. Plemmons, "Algorithms and applications for approximate nonnegative matrix factorization," *Computational Statistics Data Analysis*, vol. 52, pp. 155–173, 9 2007.
- [30] C. C. Gordon, T. Churchill, C. E. Clouser, B. Bradtmiller, J. T. McConville, I. Tebbets, and R. A. Walker, "1988 anthropometric survey of u.s. personnel: Summary statistics interim report," 1988.
- [31] G. I. Bain, N. Polites, B. G. Higgs, R. J. Heptinstall, and A. M. McGrath, "The functional range of motion of the finger joints," *Journal of Hand Surgery: European Volume*, vol. 40, pp. 406–411, 5 2015.
- [32] V. Gracia-Ibáñez, M. Vergara, J. L. Sancho-Bru, M. C. Mora, and C. Piqueras, "Functional range of motion of the hand joints in activities of the international classification of functioning, disability and health," *Journal of Hand Therapy*, vol. 30, pp. 337–347, 7 2017.
- [33] Physiotutors. (2024) Wrist/hand active range of motion (arom) — basic assessment.
- [34] J. Lachner, M. C. Nah, S. Stramigioli, and N. Hogan, "Exp[licit] an educational robot modeling software based on exponential maps," *IEEE/ASME International Conference on Advanced Intelligent Mechatronics, AIM*, pp. 1359–1366, 2024.
- [35] E. Todorov, T. Erez, and Y. Tassa, "Mujoco: A physics engine for model-based control," *IEEE International Conference on Intelligent Robots and Systems*, pp. 5026–5033, 2012.
- [36] E. R. Kandel, J. D. Koester, S. H. Mack, and S. A. Siegelbaum, *Principles of Neural Science, Sixth Edition*. McGraw Hill, 2021.
- [37] M. G. Catalano, G. Grioli, E. Farnioli, A. Serio, C. Piazza, and A. Bicchi, "Adaptive synergies for the design and control of the pisa/it softhand," *International Journal of Robotics Research*, vol. 33, pp. 768–782, 4 2014.
- [38] M. Laffranchi, N. Boccardo, S. Traverso, L. Lombardi, M. Canepa, A. Lince, M. Semprini, J. A. Saglia, A. Naceri, R. Sacchetti, E. Grupponi, and L. De Micheli, "The Hannes hand prosthesis replicates the key biological properties of the human hand," *Science Robotics*, vol. 5, no. 46, p. 467, 2020.
- [39] P. Morasso, "Spatial control of arm movements," *Experimental Brain Research*, vol. 42, pp. 223–227, 4 1981.
- [40] J. R. Flanagan and A. K. Rao, "Trajectory adaptation to a nonlinear visuomotor transformation: evidence of motion planning in visually perceived space," *Journal of Neurophysiology*, vol. 74, no. 5, pp. 2174–2178, 1995, pMID: 8592205.
- [41] P. Dizio and J. R. Lackner, "Motor adaptation to coriolis force perturbations of reaching movements: endpoint but not trajectory adaptation transfers to the nonexposed arm," *Journal of neurophysiology*, vol. 74, pp. 1787–1792, 1995.